

A 380 GHz SIS Receiver using  
Nb/AlO<sub>x</sub>/Nb Junctions for a RadioAstronomical  
Balloon-borne Experiment : PRONAOS

N 93-27742  
516-89  
160530

P. Febvre\*\*+, P. Feautrier\*\*, C. Robert\*, J.C. Pernot\*\*,  
A. Germont\*, M. Hanus\*\*, R. Maoli\*, M. Gheudin\*, G. Beaudin\*, P. Encrenaz\*\*

p 21

\**Observatoire de Paris-Meudon, DEMIRM - URA 336*

*5, Place Jules Janssen 92195 Meudon - France*

\*\* *Ecole Normale Supérieure, Laboratoire de Radioastronomie,*

*24 rue Lhomond 75005 Paris - France*

*+ Now at Jet Propulsion Laboratory*

*M.S. 168-314*

*4800 Oak Grove Drive*

*Pasadena, California 91109 USA*

## ABSTRACT

The superheterodyne detection technique used for the spectrometer instrument of the PRONAOS project will provide a very high spectral resolution ( $\Delta\nu/\nu = 10^{-6}$ ). The most critical components are those located at the front-end of the receiver : their contribution dominates the total noise of the receiver. Therefore it is important to perform accurate studies for specific components, such as mixers and multipliers working in the submillimeter wave range.

Difficulties in generating enough local oscillator (L.O.) power at high frequencies make SIS mixers very desirable for operation above 300 GHz. The low L.O. power requirements and the low noise temperature of these mixers are the primary reason for buiding an SIS receiver.

This paper will report the successful fabrication of small ( $\leq 1 \mu\text{m}^2$ ) Nb/Al-Ox/Nb junctions and arrays with excellent I-V characteristics and very good reliability, resulting in a low noise receiver performance measured in the 368/380 GHz frequency range.

## I - INTRODUCTION

Observations from a stratospheric balloon are unobstructed by the atmosphere which is opaque at submillimeter and far-infrared wavelengths from the ground. For this reason, a submillimeter balloon-borne observatory is being developed under the responsibility of the "Centre National d'Etudes Spatiales" (CNES), the French Space Agency.

It consists of a stabilized gondola supporting a 2 meter diameter telescope, associated alternately with an infrared multiband spectrometer or a submillimeter heterodyne spectrometer (SMH). This last instrument will be used to simultaneously detect the 368 GHz O<sub>2</sub> line and the 380 GHz H<sub>2</sub>O line in the interstellar medium. It is scheduled to fly in fall 1994 using a 1,000,000 m<sup>3</sup> balloon at an altitude of 37 km.

Receivers using SIS tunnel junctions have shown better sensitivities than Schottky diode receivers operated at millimeter and submillimeter wavelengths. Theoretically, sensitivities approaching the quantum limit can be achieved [1].

Up to about 300 GHz the most sensitive receivers use waveguides and superconducting RF tuning circuits integrated with the SIS junctions [2,3,4,5,6,7,8]. Above this frequency, two options appear to be available. The first possibility is to design a waveguide mixer (with full-height or reduced-height waveguide) using two tuners (i.e. generally a backshort and an E-plane tuner) [9,10]. A DSB receiver noise temperature of 150 K at 345 GHz has been reported with this design [9]. Another possibility is to use a quasioptical SIS mixer, which is very promising above 500 GHz where very small waveguides are very difficult to machine [11,12,13,14]. This design is compatible with tuning elements.

Finally we have chosen for our first experiments a waveguide design because it is better understood than open-structure mixers.

## II - RECEIVER DESCRIPTION

A block diagram of our submillimeter wave heterodyne spectrometer is shown in figure 1. Rotation of a flat mirror set allows the calibration of the receiver by commutating the incoming beam from the telescope between a hot and a cold load. Due to the short wavelengths, a quasioptical free space propagation is adopted [15]. A Mach-Zehnder type diplexer is used for the 374 GHz local oscillator signal injection into the SIS mixer. The L.O. source consists of a phase-locked 93.5 GHz Gunn diode oscillator combined with two varactor diode doublers connected in series. The intermediate frequency (I.F.) is chosen at 5.85 GHz to allow the simultaneous detection of the O<sub>2</sub> line in the lower band at 368 GHz and the H<sub>2</sub>O line in the upper band at 380 GHz. The I.F. output feeds a specially designed cooled low-noise HEMT amplifier with a gain of 30 dB. A noise temperature of 18 K has been achieved at 5.85 GHz over a 700 MHz bandwidth at a temperature of

27 K [16]. The signal is then amplified at room-temperature and coupled to the acousto optical spectrometer (AOS) subsystem with a resolution of 800 kHz in a 800 MHz bandwidth.

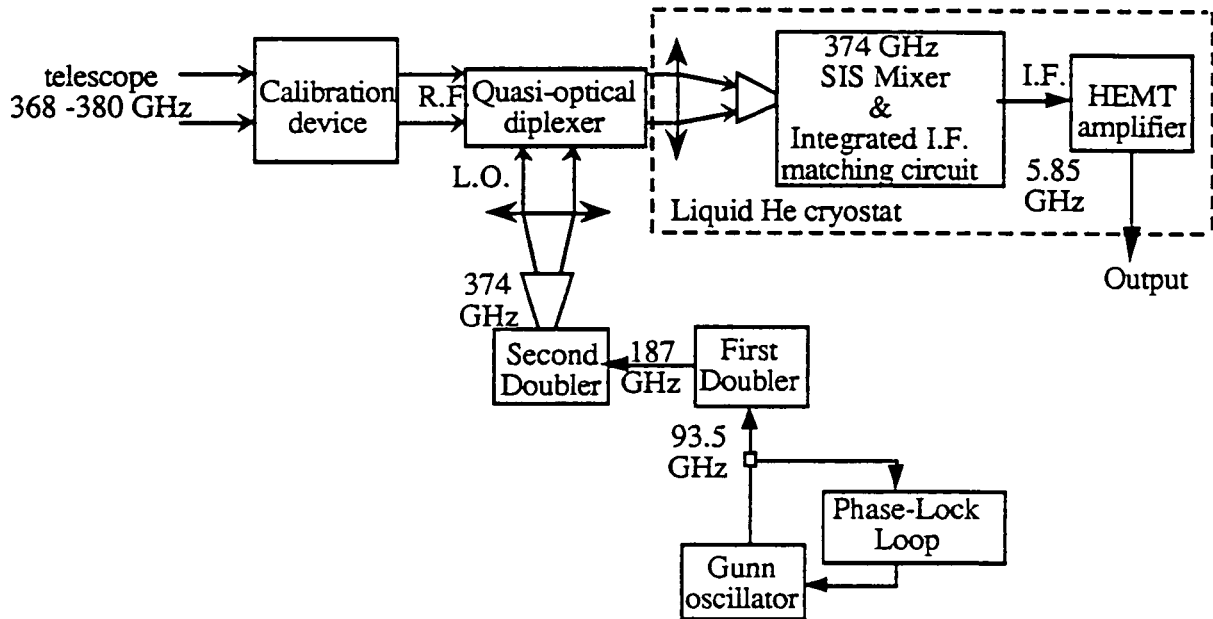


Figure 1: Block diagram of the receiver front-end used for PRONAOS

### III - 380 GHz SUBMILLIMETER RECEIVER FRONT-END

#### III-1 - SIS junctions fabrication procedure

We report here the fabrication process of Nb/Al-AlO<sub>x</sub>/Nb junctions with very sharp I-V curves and a gap voltage for one junction about 2.9 mV at 4.2 K. A high gap voltage is known to be necessary for good results at high frequencies (above 300 GHz). It is the reason why NbN junctions are promising for very high frequencies (above 500 GHz). The smallest junction area achievable with our technology without deterioration of the I-V curve is 0.9 μm<sup>2</sup>. Our process has already been described in a previous paper [17]. Some parameters have changed since this article to obtain the desired junction area for the 380 GHz mixer.

The fabrication process is described on figure 2. The Nb/Al-AlO<sub>x</sub>/Nb trilayer is deposited on the whole substrate without breaking the vacuum in order to have a good barrier interface (see fig. 2-a). The diameter of this substrate is one inch, and the thickness is 95 ± 5 μm. It is made of fused quartz and is polished on one side. During the deposition the substrate is attached to a copper heat sink cooled by a closed water circuit at 20 °C. The vacuum is made by a cryopump with a background pressure typically under 5 · 10<sup>-6</sup> Pa. The Nb and Al films are sputter deposited by a DC magnetron at an argon pressure of 1.1 Pa. The Nb base electrode (170 nm thick) and

counterelectrode (100 nm thick) are evaporated at a rate of 1.9 nm/sec. The Al film ( 10 nm ) is deposited with an oscillating substrate table at a rate of 0.2 nm/sec and is oxidized by introducing Ar + 10% O<sub>2</sub> into the chamber for 20 to 30 min at 60 to 1000 Pa.

A positive photoresist is deposited and patterned to define the RF filter with an etching technique. Nb and Al films are etched by reactive ion etching in SF<sub>6</sub>. Nb is etched with a 10 sccm SF<sub>6</sub> flow at 0.7 Pa using 60 W of power. The corresponding etching rate is 200 nm/min. Al is etched at lower pressure and higher power with an etching rate of 10 nm/min; the SF<sub>6</sub> flow is 5 sccm, the pressure is 0.3 Pa and the power is 80 W. Under these conditions, the etching is dominated by a mechanical action rather than a chemical effect like in the plasma etching method. We observed that a CF<sub>4</sub> gas does not etch Al even at low pressure. RIE with Ar has not been selected, because it produces too much damage on the resist (with Ar, it is only a mechanical etching process).

After removing the remaining photoresist in acetone (see fig. 2-b), a new resist layer is deposited to define the junction area (see fig.2-c). This is the critical point of the process which limits the smallest area achievable by this technology. Our mask aligner uses a 400 nm UV source and is limited to 0.8 μm resolution. In practice, it is impossible to define a diameter smaller than 1 μm ( ie. an area smaller than 0.9 μm<sup>2</sup> ). This resist is used to protect the upper layer of Nb etched by RIE under the following conditions : 20 sccm of SF<sub>6</sub>, 6 sccm of O<sub>2</sub>, a pressure of 0.7 Pa and a power of 60 W. If the etching rate (100 nm/min) is lower than for the trilayer etching (see fig. 2-a), these conditions provide sloped edges which are easier to insulate without microshorts in the next step. The etch stops at the Al<sub>2</sub>O<sub>3</sub>/Al barrier, because the etching rate of Al is very low with SF<sub>6</sub>/O<sub>2</sub>. We use laser end point detection to avoid overetching ( it is necessary to have a sufficient thickness of resist for the SiO lift-off ).

Once the upper Nb etched then a 300 nm layer of SiO is evaporated to insulate the junction perimeter (see fig.2-d). The excess SiO is removed in acetone (lift-off). Then, the junctions in series are connected together by a 300 nm layer of Nb sputter deposited with a rate of 1.3 nm/s through another resist stencil. The excess Nb is finally lifted-off in acetone. Different experimental investigations have been made to optimise each parameter. For example, the stresses in Nb films have been minimized by changing the Ar pressure during the sputtering step. The stresses are evaluated by optical interferometry. The Nb edge is another parameter we have studied. We succeeded in obtaining sloped edges with a reasonable selectivity by using a mixture of SF<sub>6</sub> and O<sub>2</sub> at low pressure for the RIE. Finally, anodisation spectroscopy was an useful method to investigate the quality of the interfaces Nb/Al and to understand the diffusion problem of Al into Nb; such a diffusion process gives poor quality junctions .

Then, the individual junctions ( 400 junctions per substrate of 1 inch diameter) are cut with a dicing saw and cooled in liquid helium at 4.2 K to test their I-V characteristics. It is possible to test 6 junctions in one run. The junctions are connected with spring contacts on gold pads evaporated at the ends of the R.F. filter. With this technique, we can contact the 6 junctions very quickly without problem of series resistance on Nb surface.

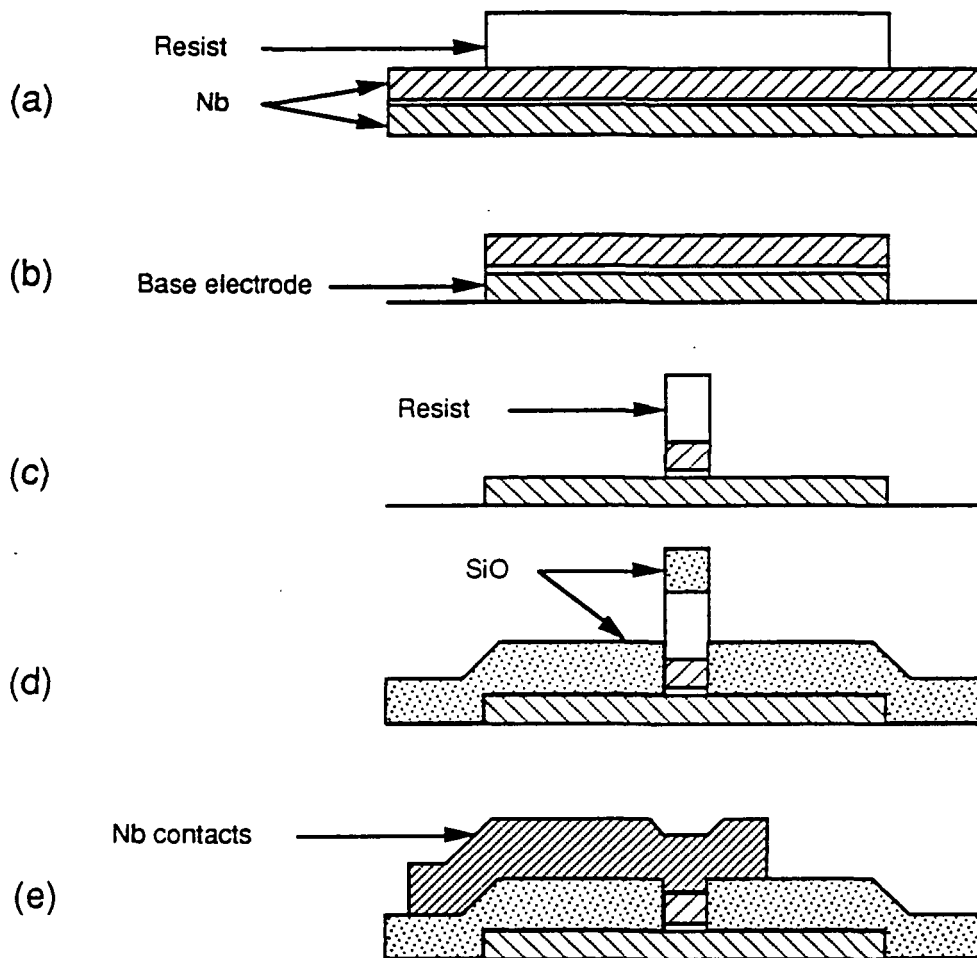


**Figure 2: Fabrication process of Nb/Al-AIOx/Nb junctions**

(a) Nb/Al-AIOx/Nb deposition. Definition of the base electrode by photolithography. (b) Etching of the trilayer. (c) Etching of the upper electrode. (d) Self-aligned deposition of a SiO insulating layer. (e) Nb interconnection layer.

Figure 3 gives an example of a typical I-V curve of an array of 2 junctions in series. The area of each junction is  $0.9 \mu\text{m}^2$ , so the effective area of the array is about  $0.45 \mu\text{m}^2$ .

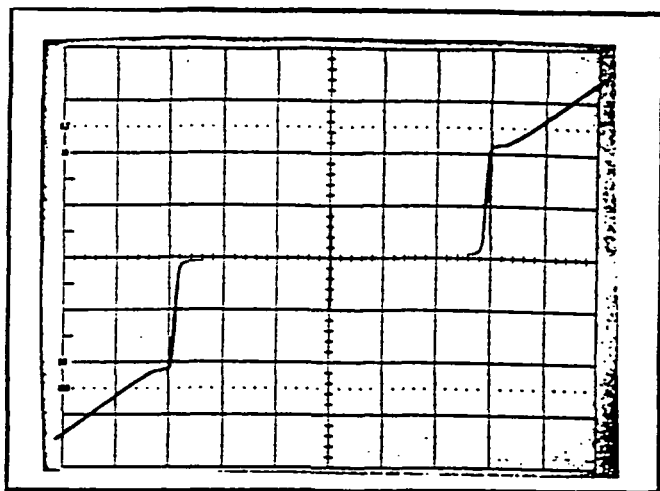


Figure 3

20  $\mu\text{A}$  / div

2 mV / div

 $A_{\text{eff}} = 0.47 \mu\text{m}^2$  $R_N = 150 \Omega$  $R_{300\text{K}} = 182 \Omega$ 

### III-2 - Mixer design

#### a) General features

The SIS mixer block is based on the Ellison design [9]. It includes an electroformed integrated dual-mode Potter horn [18] transformed by a circular to rectangular transition into a third-height reduced waveguide [19] to increase R.F. bandwidth and decrease the characteristic impedance at  $150 \Omega$ . Superconducting coils (to suppress the Josephson Current), an I.F. matching circuit and junction DC bias are integrated in the mixer block in order to facilitate the installation of the SIS mixer in the laboratory cryogenerator or in the flight cryostat. This also allows better reproducibility of mixer performance due to the optimization of the mixer mount for the SIS junctions. Dimensions of the waveguide are  $700 \mu\text{m} \times 120 \mu\text{m}$  and two contacting tuners (i.e. a backshort and an E-plane tuner placed at  $\lambda/2$  towards the feedhorn in front of the junction) provide a large range of embedding impedances to the SIS junctions (see figure 4).

#### b) Mixer configuration

A low-pass microstrip filter designed on Touchtone [20] is fabricated by photolithography on a 0.1 mm thick fused quartz substrate; its rejection is about 20 dB at 374 GHz. The metallization is made of Nb like the SIS junction and this 1.8 mm long 0.2 mm wide substrate is only put down in the mixer block channel on a thin silicon grease film for a better thermal contact. Mechanical support is provided by this silicon grease film when cooled at 4 K and by the  $25 \mu\text{m}$  gold wires contacting the filter to ground and the L.F. output. This assembly allows numerous tries of different junctions without breaking substrates. The I.F. output gold wire is fixed with silver glue on the low-pass filter at one end and directly on the I.F. matching circuit at the other end. This matching circuit formed on Duroïd ( $\epsilon_r = 10.2$ ) supports the junction DC bias too. This avoids the sudden impedance change of a SMA connector, increases the I.F. bandwidth and decreases the I.F. losses. The DC bias includes two  $10 \text{ k}\Omega$  chip resistors (to prevent junction from being destroyed by voltage spikes) followed by an insulated wire soldered at  $\lambda/4$  of a  $\lambda/2$  stub (see figure 5) to provide approximately an open circuit at the I.F. frequency of 5.85 GHz on a 700 MHz bandwidth. The

25  $\mu\text{m}$  gold wire is the first part of the I.F. matching circuit, then a length of a microstrip line provides a real impedance transformed into  $50 \Omega$  by a  $\lambda/4$  line (figure 5).

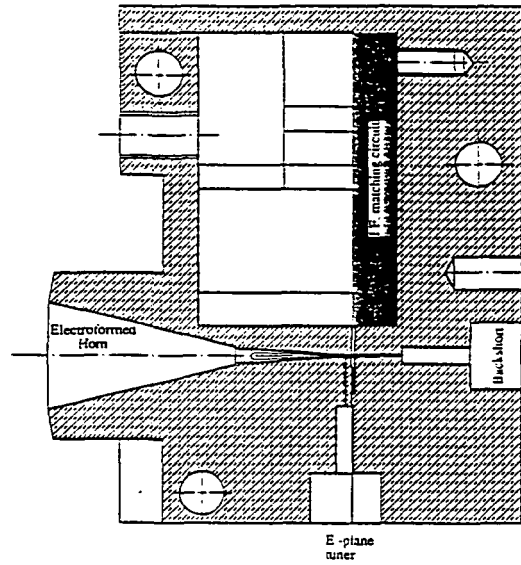


Figure 4

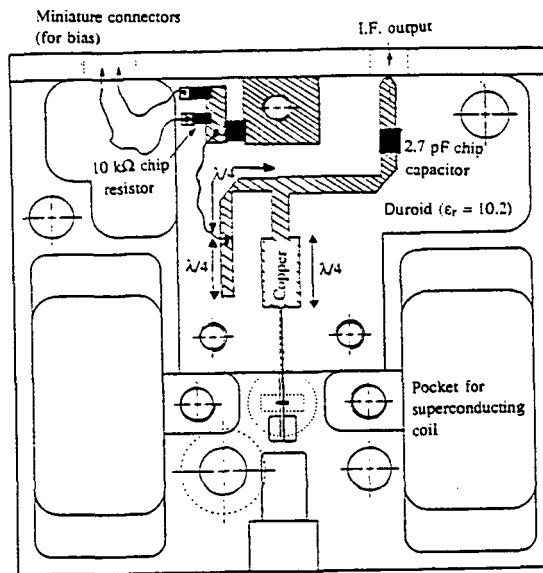


figure 5

The 1.8 cm diameter superconducting coils have been designed to produce 310 Gauss with a current of 1 A. Each one is made of about 1200 turns of Niobium-Titanium superconducting wire. Indeed, for circular junctions of surface  $S$ , the magnetic field suppressing the Josephson current is given by :

$$B(\text{Gauss}) = \frac{2,23 \cdot 10^{-11}}{d \cdot \sqrt{S}} \quad (\text{for one flux quantum})$$

with :  $d = 2\lambda_L + w$  where:

$\lambda_L$  = London penetration depth of Nb (m)

$w$  = width of insulator between the two superconductors (m)

The area of the smallest junctions fabricated in the laboratory is about  $1 \mu\text{m}^2$ . So, with a pessimistic value of the London penetration depth ( $400 \text{ \AA}$ ),  $B = 255 \text{ Gauss}$  ; the real value should be lower. The coils are small, because the flight cryostat was specified for a smaller Schottky mixer. Moreover, some constraints about the optical axis were already fixed in the flight cryostat. The mixer block is a Faraday cage for these coils against electromagnetic spikes even if any external magnetic field can penetrate into it .

#### IV - LABORATORY MEASUREMENT BENCH

Results shown further have been obtained on a laboratory bench with a 4 K cryogenerator including two closed circuits of helium. The first one is a classical CTI 1020 compressor including two stages at 50 K and 12 K. The second one is a Joule-Thomson expansion pumping on the 12 K stage to reach 3 to 4 K on the "4 K" stage. Temperature can be quickly changed and stabilized by varying the return helium pressure of the 4 K helium circuit [21]. A teflon corrugated window is used on the room temperature shield for the quasioptical RF input. The heat flux entering the cryogenerator is then reduced with an IR filter. It's a  $80 \mu\text{m}$  thick (one wavelength at 374 GHz) 48 mm diameter crystalline quartz plate mounted on the 50 K stage shield. Then a 0.8 mm thick fluorogold window, 38 mm diameter, filters the far IR 50 K blackbody radiations. The SIS mixer is on the 4 K stage at the focus of a cold corrugated teflon lens cooled by the same stage.

Mechanical contacting tuners are operated by vacuum feedthroughs and are manually movable with micrometer drives when measuring receiver performance. Each electrical wire, I.F. cable or tuner drive is thermalized at 12 K and 50 K to exhaust heat flows. Some miniature connectors are used for the DC bias. A four points measurement of the I-V curve releases us from any series resistance.

The I.F. output of the SIS mixer is connected to a semi-rigid cable followed by a coupler, an isolator and the HEMT amplifier. This low-noise amplifier is installed on the 12 K stage, its output cable is thermalized at 50 K before going out of the cryogenerator (see figure 6). The coupler is



used to inject an additive noise at the I.F. mixer output to know its match relatively to  $50 \Omega$ . A preliminary calibration without mixer allows us to calculate approximatively the mixer temperature  $T_M$  and its conversion losses  $L_M$ .

The socket of the superconductive coils is installed on the 12 K stage to have a better thermal contact between superconducting and copper wires and to prevent a heating of the 4 K stage. The L.O. and signal injections are achieved by a quasi-optical diplexer. The coupling ratio for the L.O. is higher than 90 %.

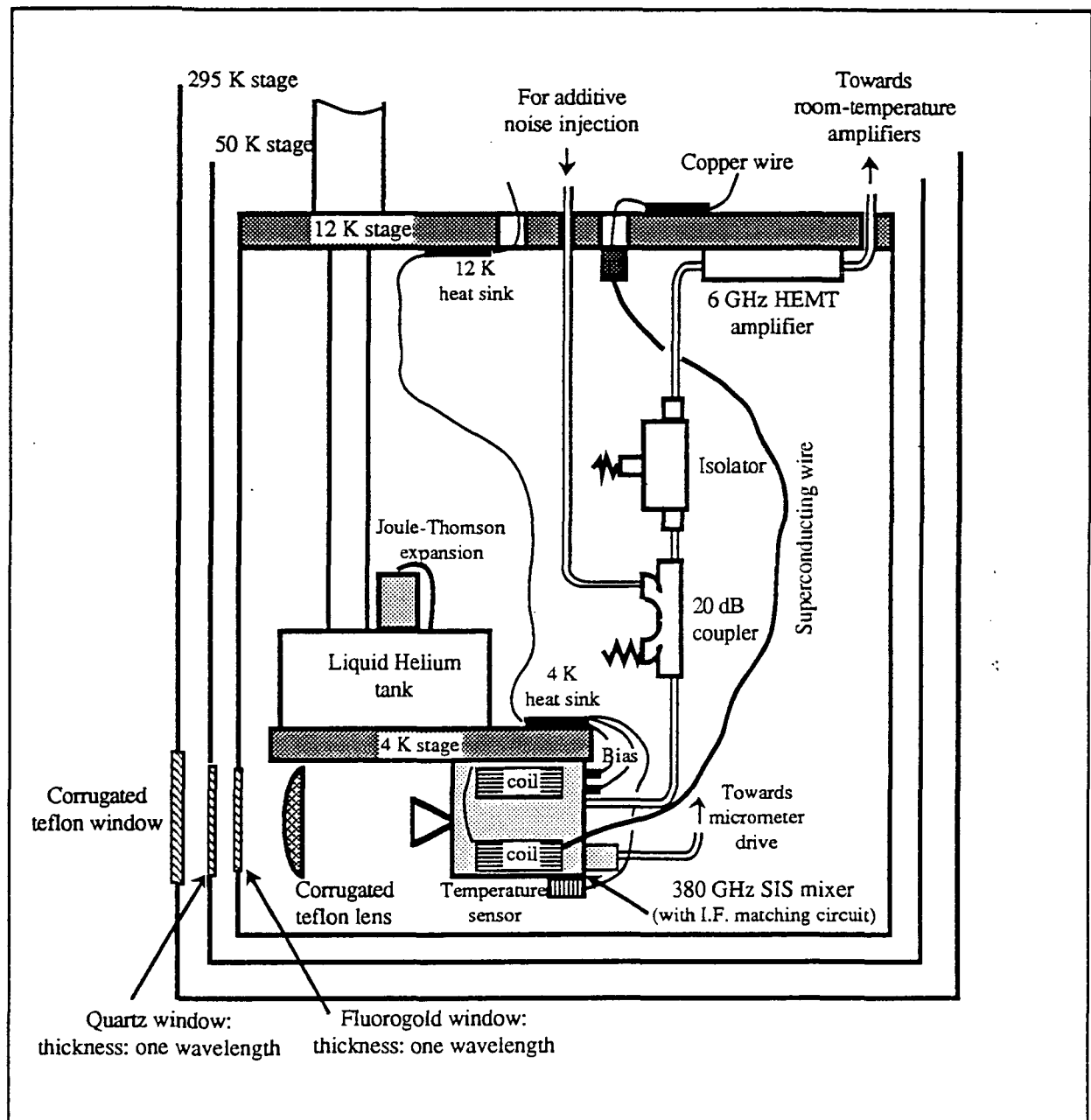


Figure 6

## V - LOCAL OSCILLATOR VARACTOR DIODE DOUBLERS

The structure of each doubler has already been described in a previous paper [22]. The maximum efficiency found for the first doubler was about 18 % for an incident power of 15 mW with a 5P8 diode of the University of Virginia. The input frequency was 91.6 GHz and the output power was higher than 6 mW with a 50 mW input power. These results haven't been found again with the other doubler block at 93.5 GHz. They were due to a very good coupling between the diode and the waveguide by the whisker. More commonly, we can reach 3 to 4.5 mW with a good reproducibility and with an input power of 50 mW at 93.5 GHz. A typical curve of our last results is shown on figure 7.

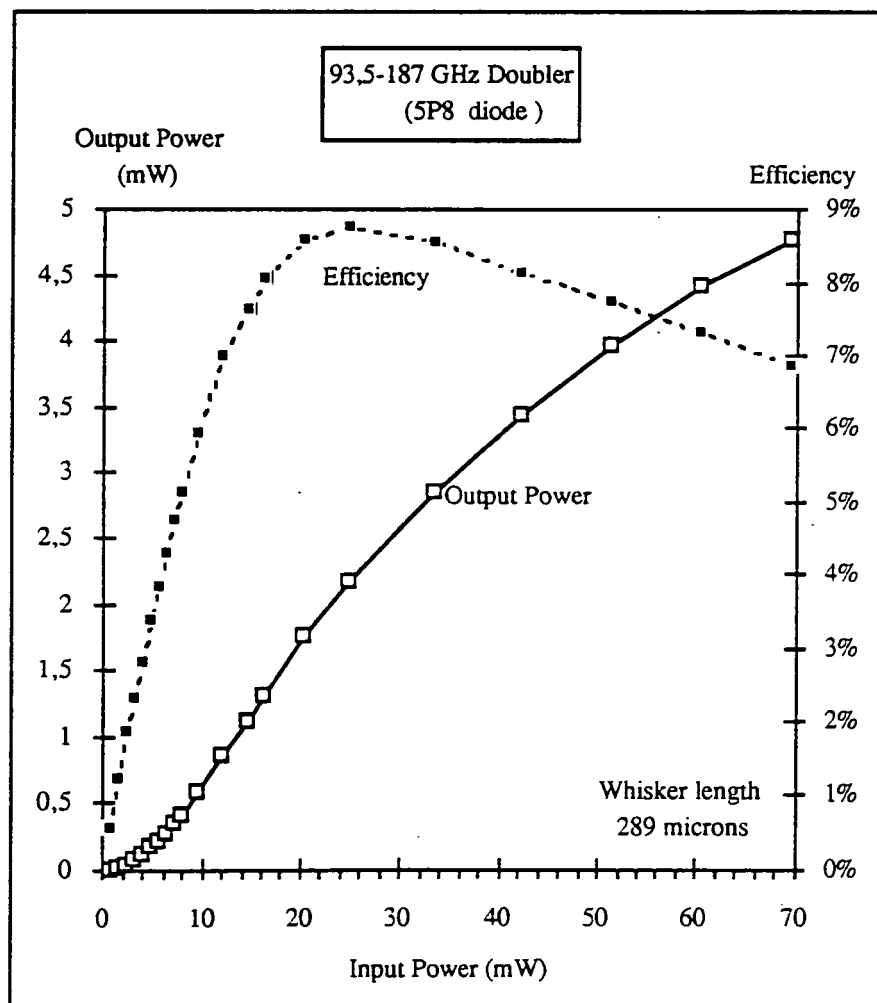


Figure 7

Concerning the second doubler, its input power (approximately the output power of the first doubler) is low and consequently its efficiency is relatively low. Indeed, we can see on

figure 7 that the efficiency of the first doubler is lower than 4 % at 187 GHz for an input power of about 5 mW.

Partly due to the much higher frequency, we can foresee that the second doubler will not produce so much power. Such a local oscillator cannot be used for a Schottky mixer. Nevertheless, some diodes whose the maximum efficiency is obtained for a 3-4 mW input power like bbBNN diodes could provide sufficient power to pump a Schottky mixer [23]. The best output power obtained at 374 GHz is approximately 30  $\mu$ W with the bolometer horn put directly across from the second doubler horn, i.e. an efficiency lower than 1%. Two types of diodes have been tested, 2T8 and 2T9, they come from the University of Virginia and we can see on the following figure 8 that the 2T8 diode provides more power than the 2T9 diode. This is partly due to its smaller capacitance (4 fF versus 8 fF for the 2T9 diode).

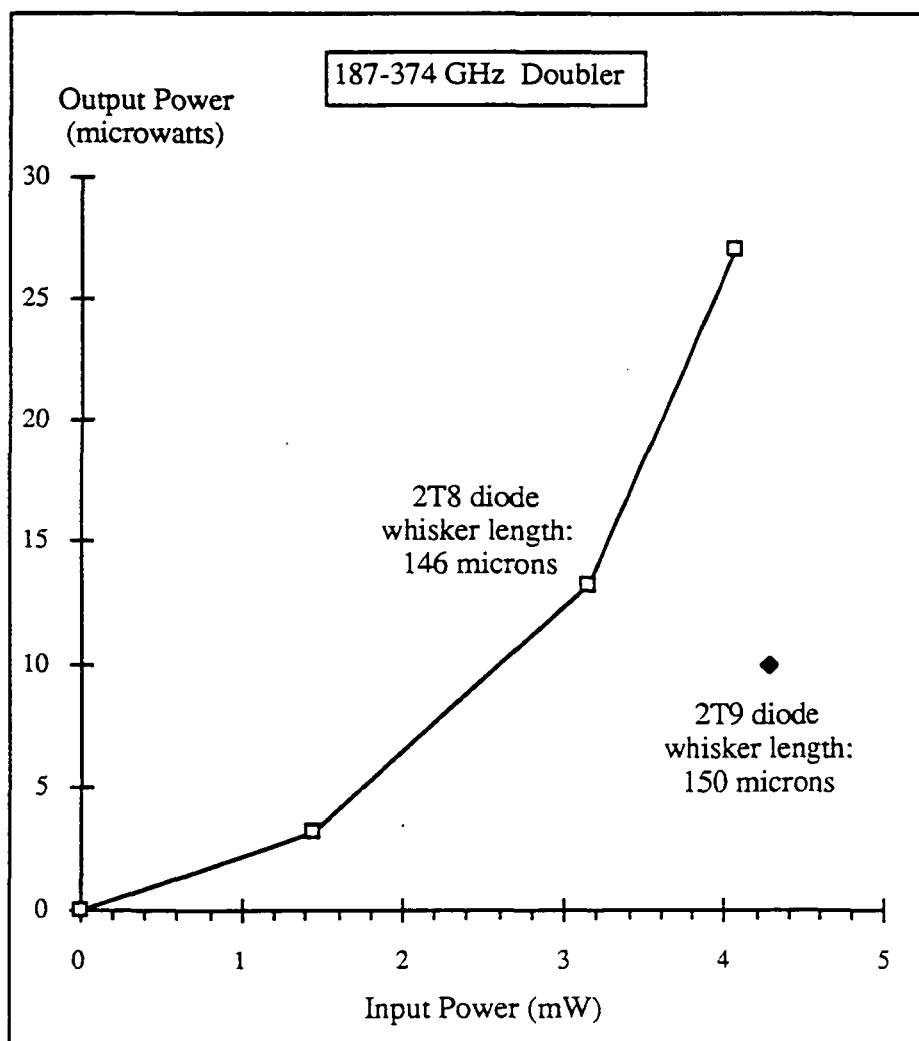


Figure 8

To prevent the second doubler diode from being destroyed by voltage spikes and due to the low input power, it has been short circuited in direct current instead of being reverse biased for an optimum efficiency, this diminishes the output power. Moreover, input and output backshorts of each doubler have been fixed or soldered which still damages performance. So the output power at 374 GHz is about 13  $\mu\text{W}$ . Other measurements have been made with a quasi-optical bench composed of two corrugated lenses which is approximately the bench used for the measurements of the SIS mixer. The output power is then 10  $\mu\text{W}$ . This local oscillator signal is powerful enough, even to pump four SIS junctions in series.

## VI - RESULTS

Different types of junctions have been tested with 2, 3 or 4 junctions in series coming from the same wafer. The best results obtained with each substrate are summarized in table I. The L.O. frequency is 374 GHz, the I.F. center frequency is 5.85 GHz. Measurements have been made with a 285 MHz I.F. bandwidth filter, we used the Y-factor method with 2 loads at 77 K and 295 K.

□ We can firstly point out the good match between calculated and measured values of the magnetic field suppressing the Josephson current  $I_J$ . The product  $B(I_J = 0) \times D$  is reported on the following table II (for one flux quantum), where  $B(I_J = 0)$  is the magnetic field suppressing the Josephson current and  $D$  the diameter of one junction. This product should be constant for junctions fabricated on the same wafer according to the previous formula of III-2-b:  $d$  is a parameter depending only on the oxidation time of aluminium in  $\text{Al}_2\text{O}_3$ . We see that  $B(I_J=0) \times D$  is nearly constant to within about 10 %, this comes from the uncertainty of the junction areas. We can also deduce the London penetration depth of our niobium films which is about 600 Å.

□ Nevertheless, the Josephson Current is not always completely suppressed with one flux quantum, because the areas of the junctions in series are slightly different. The Josephson current for each of the couple of junctions in series of one substrate is reported on figure 9.

The relative difference of the magnetic field suppressing the Josephson Current of each junction taken individually is about 5 to 10 %, that means a relative difference of area between the two junctions of 10 to 20 %. Such a difference is in good agreement with the accuracy of photolithography to define small junction areas. For this reason, the current densities and the  $\omega R_{\text{NC}}$  products are not exactly the same for the different junctions of the table I. This corresponds to the uncertainty of the value of the junction area.

□ The measurements of the required L.O. power are deduced from a preliminary calibration of the L.O. output power as a function of the first doubler self-biased voltage. The required power depends on the square of the number of junctions in series; four junctions in series should require

about four times as much power as two junctions in series. We observed a 3.7 dB difference between expected and measured values which corresponds mainly to the R.F. mismatch at the 374 GHz frequency since we measured the incoming L.O. power. And we can see that the difference of the conversion losses for these junctions is 3 dB, this point confirms the first one.

| Junction                              | E380-1-8-2          | E380-1-6-5             | E380-1-8-4     | E380-1-4-1             | E380-1-8-6     |
|---------------------------------------|---------------------|------------------------|----------------|------------------------|----------------|
| Diameter ( $\mu\text{m}$ )            | 1.1                 | 1.5                    | 1.1            | 1.9                    | 1.1            |
| Number of junctions in series         | 2                   | 3                      | 2              | 4                      | 2              |
| Effective surface ( $\mu\text{m}^2$ ) | 0.47                | 0.59                   | 0.47           | 0.71                   | 0.47           |
| $R_N(\Omega)$                         | 143                 | 137                    | 150            | 113                    | 143            |
| $\omega R_N C$ at 374 GHz             | 9.5                 | 11.4                   | 10             | 11.3                   | 9.5            |
| $j_c$ ( $\text{A}/\text{cm}^2$ )      | 4600                | 3600                   | 4600           | 4200                   | 4400           |
| L.O. power ( $\mu\text{W}$ )          | ?                   | ?                      | ?              | 7.5                    | 0.8            |
| Magnetic field applied (Gauss)        | 175                 | 255<br>(2 flux quanta) | 175            | 192<br>(2 flux quanta) | 185            |
| DSB receiver temperature (K)          | 1200                | 470                    | 360            | 525                    | 310            |
| Mixer noise temperature $T_M$ (K)     | ?                   | 200                    | 195            | 225                    | 155            |
| Conversion losses (dB)                | ?                   | 11                     | 9,1            | 11,8                   | 8,8            |
| Transmitted I.F. power                | between 10 and 40 % | $\approx 90\%$         | $\approx 90\%$ | $\approx 98\%$         | $\approx 97\%$ |
| Contribution of amplifier to noise    | $> 70\%$            | 57 %                   | 46 %           | 57 %                   | 50 %           |

table I

| Junction   | E380-1-8-2 | E380-1-6-5 | E380-1-8-4 | E380-1-4-1 | E380-1-8-6 |
|--|------------|------------|------------|------------|------------|
| $B(I_J = 0) \times D$<br>(Gauss $\times \mu\text{m}$ ) | 193        | 191        | 193        | 182        | 203        |

table II

□ Relatively high conversion losses result in a contribution of 50 % for the HEMT amplifier in the receiver noise temperature. These conversion losses include intrinsic conversion losses increased by RF quasioptical injection, RF and I.F. mismatches, RF filter and I.F. matching circuit losses. Differences of receiver noise are mainly due to miscellaneous conversion losses. Indeed, some different effective areas of junction have been tested and the couple of tuners don't enable to completely tune out the junction capacitance because the  $\omega R_N C$  product is high ( $>8$ ). So the excess of conversion losses corresponds to a higher RF mismatch.

Some typical curves of different measured junctions are shown on figure 10.

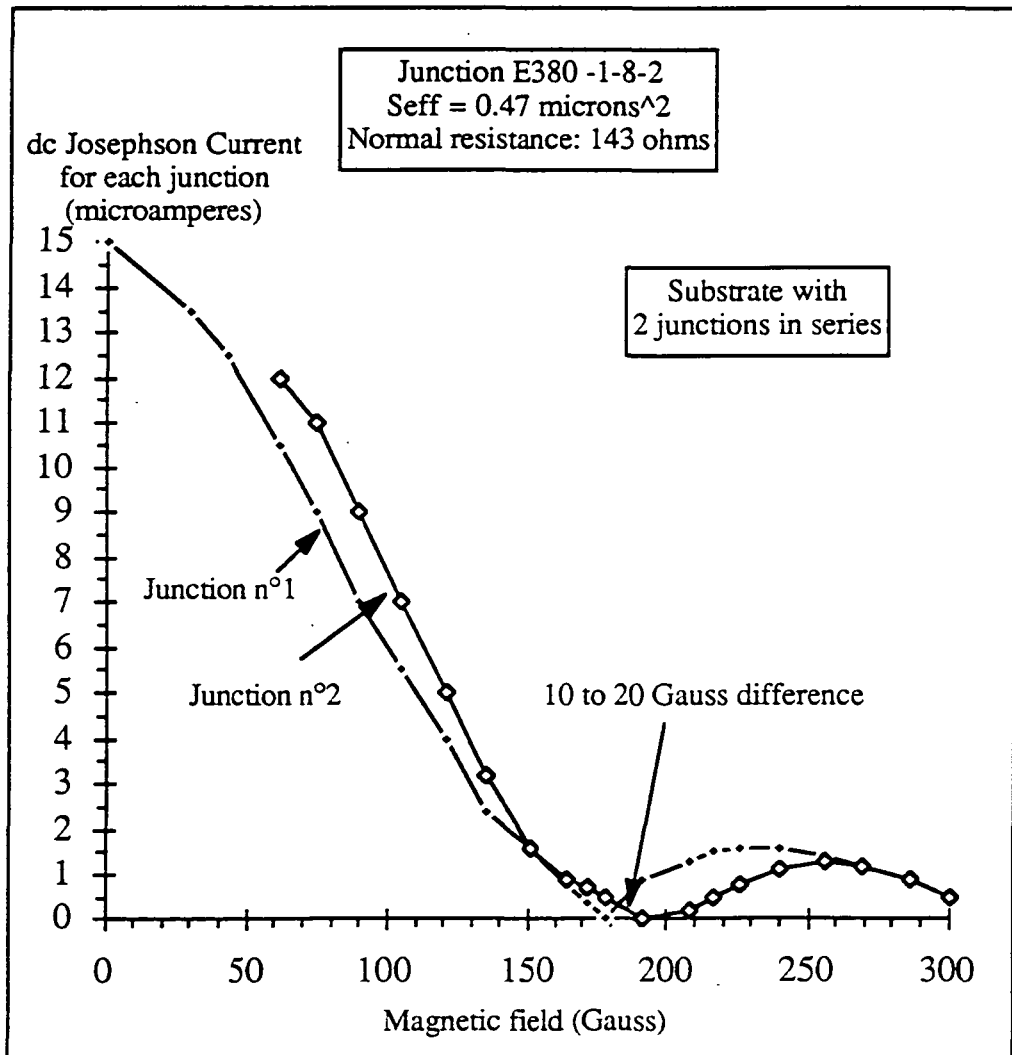


figure 9

Remark : Exact values of magnetic fields haven't been measured but calculated with current flowing through the coils. Error is around  $\pm 5 \%$ .

The three curves shown below are some experimental curves digitalized by our data acquisition system of different arrays of SIS junctions in series fabricated on the same wafer with nearly the same normal resistances (about 150 Ω). For this reason, the current densities are of the same order of magnitude for each array.

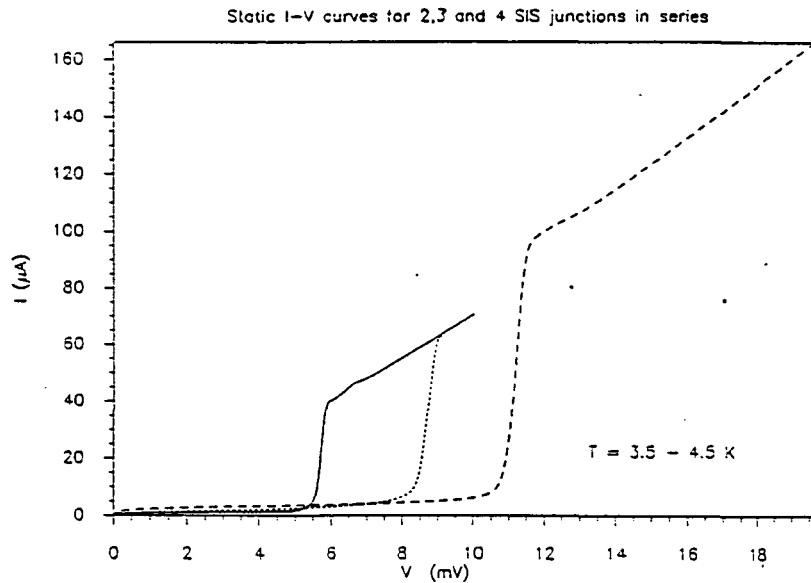


figure 10

We can see on figure 11 the dc characteristic of the junction E380-1-8-6 (a). Also shown on this figure is the I-V curve of the same junction pumped with the 374 GHz L.O.. The width of the photon assisted step is  $2 \cdot h \cdot \nu_{L.O} / e$  where  $h$  is the Planck constant,  $e$  is the electron charge and  $\nu_{L.O}$  is the frequency of the local oscillator.

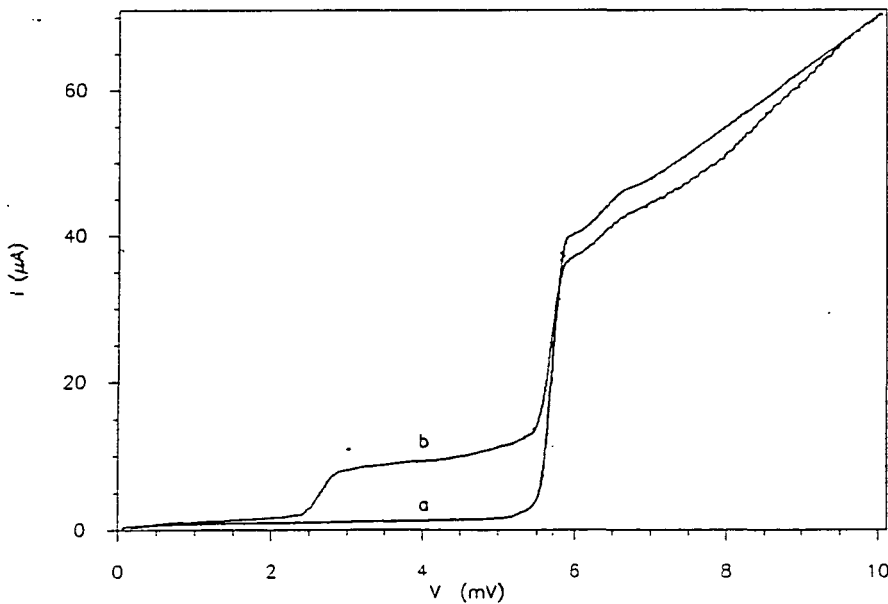


figure 11

The static impedance at the bias point (approximately 4 mV: the middle of the first photon step) is about  $500 \Omega$  so the I.F. circuit has been designed to match this impedance, we assumed that it is close to the impedance at 5.85 GHz ( $R_{I.F.}$ ). The normal resistance is  $143 \Omega$  and the range of the quotient  $R_{I.F.}/R_N$  has been found to be contained between 3 and 4.5, the value of  $R_{I.F.}$  being adjusted by varying the L.O. power. We can see in table I that the I.F. match for the last four junctions is good which validates our assumption.

On the contrary the high receiver noise temperature measured for the first junction was due to a poor I.F. match, the I.F. impedance being unknown at that time.

Some I-V curves with and without suppression of the Josephson current are plotted on the following figure 12. We can observe 3 Shapiro steps due to the coupling of the L.O. power with the Josephson current when it is not suppressed. The width of these steps is exactly one half of the quasiparticle step due to the L.O. power. These sharp steps partly explain the instabilities observed when the Josephson current is not completely suppressed.

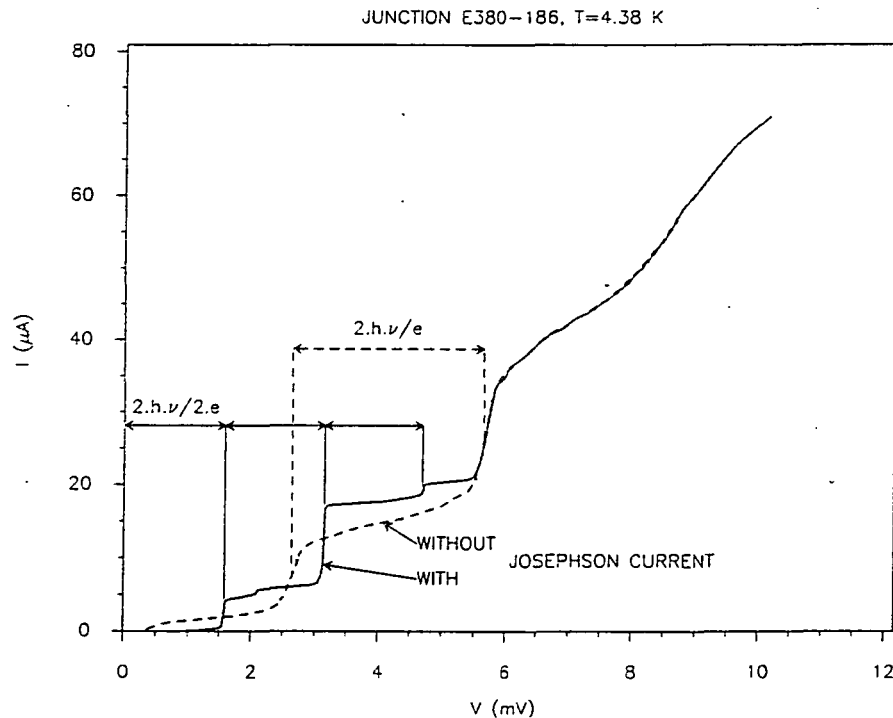


figure 12

Some dependences of different parameters are shown on the following figures. We can see on figure 13 the influence of the magnetic field to the noise receiver.

The noise temperature begins to increase for a magnetic field lower than 170 Gauss which corresponds to a residual Josephson Current of about  $1 \mu\text{A}$  providing an additive Josephson noise coming with instabilities of the I.F. output power.



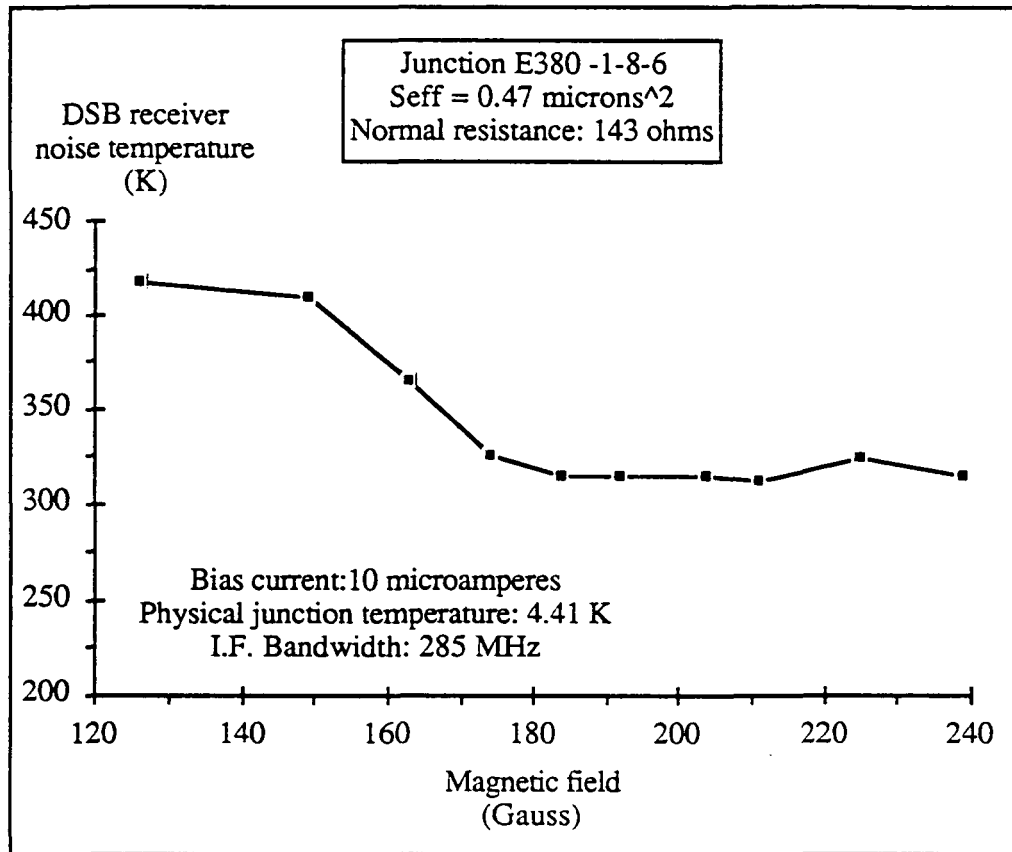


figure 13

The noise temperature is plotted as a function of bias current on figure 14. The receiver noise temperature remains lower than 330 K with a relative variation of bias current of 20 % which is adequate for our balloon-borne experiment where there is no remote control of the DC bias; all the other parameters remained unchanged.

At last, the L.O. frequency was varied from 345 to 385 GHz (see figure 15) the receiver noise temperature is higher at lower and higher frequencies than 374 GHz. This is partly due to the narrow RF bandwidth of the Potter horn. We can point out that the receiver temperature is below 380 K in the frequency range from 355 to 385 GHz.

Influence of temperature was only observed with the junction E380-1-6-5. With other junctions, the mixer noise temperature has not decreased by cooling more the junction; this is certainly due to a poor thermal contact with the silicon grease film.

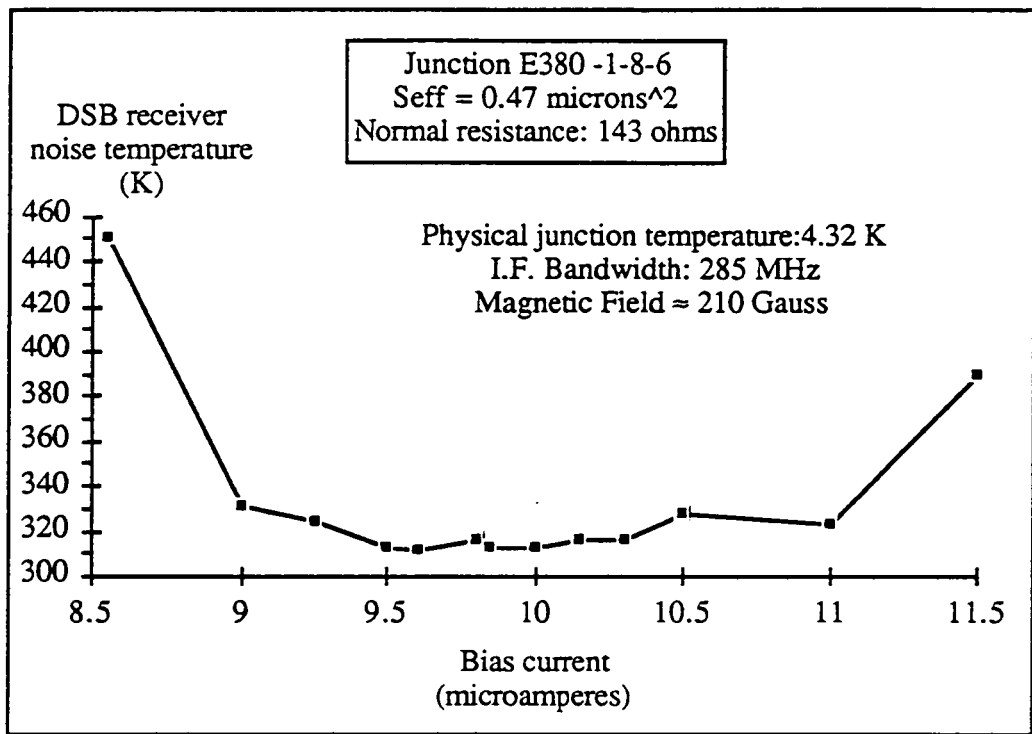


figure 14

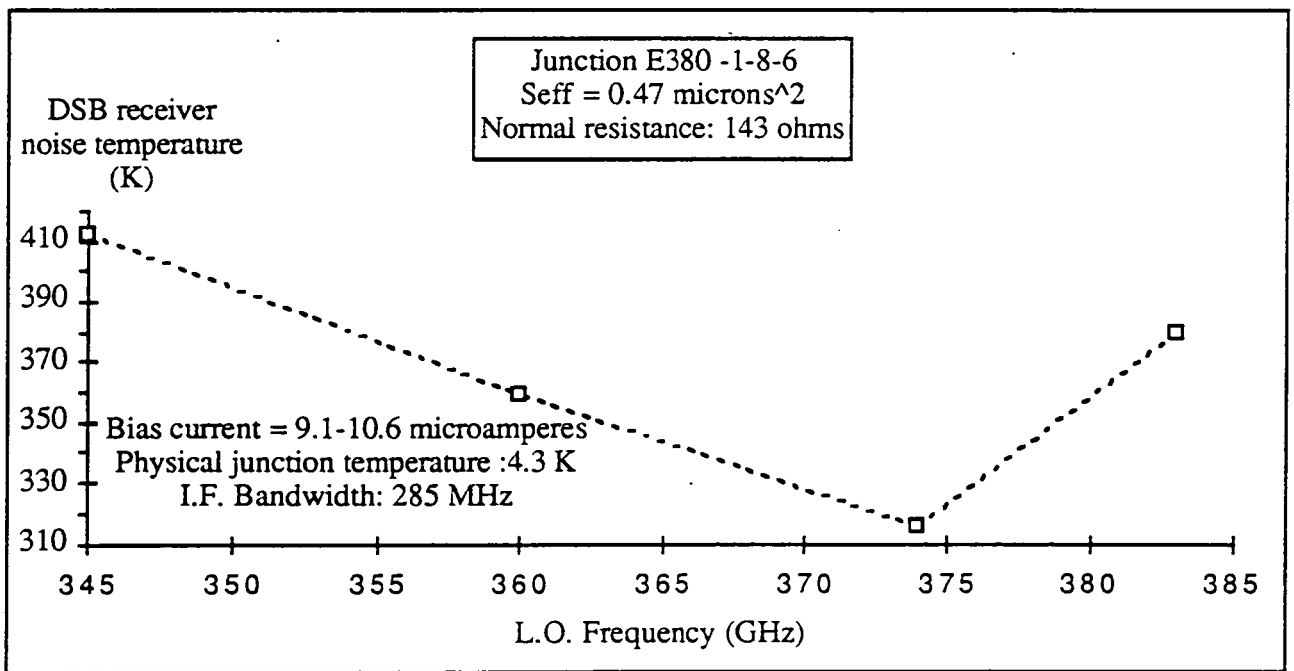


figure 15

## V - CONCLUSION

Some Nb/Al-Al<sub>2</sub>O<sub>3</sub>/Al SIS junctions with small areas and sharp I-V curves have been successfully fabricated, dc measured and integrated in the mixer. The smallest area achievable with our process is about 0.9  $\mu\text{m}^2$ . Arrays of two junctions with this area have been made, the effective area is then around 0.45  $\mu\text{m}^2$ . They are very stable according to some repeated thermal cycles: more than 15 cycles have been completed between room temperature and 4 K temperature and no change has been detected. This reliability is essential for space applications.

The 380 GHz SIS mixer was designed with an integrated I.F. matching circuit and two integrated superconducting coils; it has been tested over a 40 GHz L.O. bandwidth. The best receiver noise temperature (310 K DSB) has been measured with an array of a couple of junctions in series having an effective surface of 0.47  $\mu\text{m}^2$  and a normal resistance of 143  $\Omega$ . The L.O. frequency was 374 GHz. The relatively high conversion losses (8.8 dB) reveal a R.F. mismatch. It could be decreased by using junctions with lower capacitances (i.e. areas) and lower normal resistances. Then the fabrication of SIS junctions with higher current densities is planned. The lowest mixer noise temperature is around 155 K and some new junctions with lower normal resistances should also reduce it. So we are optimistic for the following.

The 374 GHz L.O. source has been made with a fundamental InP Gunn Oscillator at 93.5 GHz followed by two GaAs varactor doublers in series. This subsystem provides enough power to drive the SIS mixer even with 4 junctions in series but a more powerful first multiplier will be necessary to produce more power at higher frequencies (above 500 GHz) for the future.

A 6 GHz low-noise H.E.M.T. amplifier has been specifically designed for cryogenic applications, it meets fully the specifications and will be used in connexion with the SIS mixer. The contribution of the amplifier to the system noise is about 50 % due to the high conversion losses. We hope that the new junctions will decrease this contribution.

**Acknowledgments** : We would like to thank Gilles Ruffié for his valuable aid and support, André Deschamps for the data acquisition system and Olivier Perrin for the design of the doubler blocks. We are especially grateful to Serge Lebourg and Jean Morin for their help on the mechanical realizations for the measurement bench. We also wish to thank Véronique Serpette (Observatoire de Paris) for the numerous photolithographies of the I.F. matching circuits. In addition we thank Marc David for his assistance and support on cryogeny. Thanks also to Albert Brel, Annick Gassais and Françoise Gadéa for their technical help. We would also like to thank Matthew Carter and Jacques Blondel of IRAM (Institut de Radioastronomie Millimétrique) for useful discussions. Finally we are greatly indebted to William R. McGrath for his careful reading and numerous comments on this article.

This work is supported by the Centre National d'Etudes Spatiales (CNES) and the C.N.R.S. (URA 336)

## REFERENCES

- [1] J.R. Tucker: "Quantum limited detection in tunnel junction mixers", *IEEE J. Quantum Electron*, vol QE 15, pp 1234-1258, Nov. 1979
- [2] S.K. Pan, A.R. Kerr, M.J. Feldman, A.W. Kleinsasser, J.W. Stasiak, R.L. Sandstrom and W.J. Gallagher: "A 85-116 GHz SIS receiver using inductively shunted edge junctions", *IEEE Trans. MTT*, Vol.37, N° 3, March 1989
- [3] A.R. Kerr, S.K. Pan: "Some recent developments in the design of SIS mixers", *Int. J. of Infrared and Millimeter Waves*, Vol.11, N° 10, 1990
- [4] R. Blundell, M. Carter and K.H. Gundlach: "A low-noise SIS receiver covering the frequency range 215-250 GHz", *Int.J. of Infrared and Millimeter Waves*, Vol 9, N°4, 1988
- [5] B.N. Ellison and R.E. Miller: "A low-noise 230 GHz SIS receiver", *Int.J. of Infrared and Millimeter Waves*, Vol.8, pp 609-625, June 1987
- [6] H.H.S. Javadi, W.R. McGrath, S.R. Cypher, B. Bumble, B.D. Hunt and H.G. Leduc: "Performance of SIS mixers at 205 GHz employing submicron Nb and NbN tunnel junctions", *Digest of the 15th International Conference on Infrared and Millimeter Waves*, December 1990
- [7] D. Winkler, W.G. Ugras, A.H. Worsham and D.E. Prober, N.R. Erickson and P.F. Goldsmith: "A full-band waveguide SIS receiver with integrated tuning", *IEEE Trans. on Magnetics*, vol.27, n°2, March 1991
- [8] J.W. Kooi, M. Chan, T.G. Phillips, B. Bumble and H. G. Leduc: "A low-noise 230 GHz heterodyne receiver employing 0.25  $\mu\text{m}^2$  Area Nb/AlOx/Nb tunnel junctions", 2<sup>nd</sup> International Symposium on Space Terahertz Technology, Jet Propulsion Laboratory, California Institute of Technology, Pasadena, Feb. 1991
- [9] B.N. Ellison, P.L. Schaffer, W. Schaal, D. Vail, R.E. Miller: "A 345 GHz SIS receiver for radio astronomy", *Int.J. of Infrared and Millimeter Waves*, Vol. 10, N° 8, 1989
- [10] C.E. Honingh, M.M.T.M. Dierichs, H.H.A. Schaeffer, T.M. Klapwijk and Th. de Graauw: "A 345 GHz waveguide mixer with two mechanical tuners using an array of four Nb-Al-Al<sub>2</sub>O<sub>3</sub>-Nb SIS junctions", 2<sup>nd</sup> International Symposium on Space Terahertz Technology, Jet Propulsion Laboratory, California Institute of Technology, Pasadena, Feb. 1991
- [11] M. Wengler, D.P. Woody, R.E. Miller, T.G. Phillips: "A low noise receiver for millimeter and submillimeter wavelengths", *Int. J. of Infrared and Millimeter Waves*, Vol. 6, pp 697-706, 1985
- [12] T.H. Buttgenbach, R.E. Miller, M.G. Wengler, D.M. Watson, T.G. Phillips: "A broad-band low-noise SIS receiver for submillimeter astronomy", *IEEE Trans. MTT*, Vol. MTT 36, pp 1720-1726, Dec. 1985
- [13] X. Li, P.L. Richards, F.L. Lloyd, "SIS quasiparticle mixers with bow-tie antennas", *Int. J. of Infrared and Millimeter Waves*, Vol. 9, pp 101-103, 1988
- [14] J. Zmuidzinas, H.G. Leduc, "Quasi-optical slot antenna SIS mixers", to be published in *IEEE Trans. MTT*, 1992 and 2<sup>nd</sup> International Symposium on Space Terahertz Technology, Jet Propulsion Laboratory, California Institute of Technology, Pasadena, Feb. 1991
- [15] P.F. Goldsmith, "Quasi-optical techniques at millimeter and submillimeter wavelengths", *Infrared and Millimeter Waves* vol 6 : System and components, K.J. Button (editor), Academic Press, New York, p 277-343, 1982.

- [16] C.Robert, M.Gheudin: " A 6 GHz HEMT low-noise cooled amplifier for a radioastronomical submillimeter heterodyne receiver ", 15th International Conference on Infrared and Millimeter Waves, Conference digest, pp. 127-128, Orlando, dec. 1990.
- [17] P.Feautrier, J.Blondel, M.Hanus, J.Y.Chenu, P.Encrenaz, M.Carter : "Low noise 80-115 GHz quasiparticle mixer with small Nb/Al-Oxyde/Nb tunnel junctions", Int. J. of Infrared and Millimeter Waves, Vol. 11, No. 2, 1990 .
- [18] H.M. Pickett, J.C. Hardy and J. Farhoomand: "Characterization of a Dual-Mode Horn for Submillimeter Wavelengths", IEEE Trans. on MTT, vol. MTT-32,N°8, August 1984
- [19] Mixer block constructed by Radiometer Physics, Meckenheim, Germany
- [20] Touchtone CAD Software, Eesof
- [21] J.C.Maréchal, J.C.Pernot, P.J.Encrenaz: "A 2K closed cycle cryogenerator", Conf. URSI, Granada, Sept. 1984.
- [22] O.Perrin, C.Robert, P.Feautrier, P.Febvre, G.Beaudin, P.Encrenaz, M.Gheudin, J.Lacroix, G.Montignac : "380 GHz receiver front-end for the balloon-borne radioastronomical experiment PRONAOS", 2nd. International Symposium on Space Terahertz Technology, Jet Propulsion Laboratory, California Institute of Technology, Pasadena, feb. 1991 .
- [23] T.J.Tolmunen, M.A. Frerking: "Theoretical performances of novel multipliers at millimeter and submillimeter wavelengths", Int. J. of Infrared and Millimeter Waves, Vol. 12, No. 10, 1991.